New Resolution Strategy for Multi-scale Reaction Waves using Time Operator Splitting and Space Adaptive Multiresolution: Application to Human Ischemic Stroke*

Max Duarte[1,**], Marc Massot[1], Stéphane Descombes[2], Christian Tenaud[3] Thierry Dumont[4], Violaine Louvet[4], and Frédérique Laurent[1]

[1] Laboratoire EM2C - UPR CNRS 288, Ecole Centrale Paris, Grande Voie des Vignes, 92295 Chatenay-Malabry Cedex, France
[2] Laboratoire J. A. Dieudonné - UMR CNRS 6621, Université de Nice - Sophia Antipolis, Parc Valrose, 06108 Nice Cedex 02, France
[3] LIMSI - CNRS, B.P. 133, Campus d'Orsay, 91403 Orsay Cedex, France
[4] Institut Camille Jordan - UMR CNRS 5208, Université de Lyon, Université Lyon 1, INSA de Lyon 69621, Ecole Centrale de Lyon, 43 Boulevard du 11 novembre 1918, 69622 Villeurbanne Cedex, France

Abstract. We tackle the numerical simulation of reaction-diffusion equations modeling multi-scale reaction waves. This type of problems induces peculiar difficulties and potentially large stiffness which stem from the broad spectrum of temporal scales in the nonlinear chemical source term as well as from the presence of large spatial gradients in the reactive fronts, spatially very localized. In this paper, we introduce a new resolution strategy based on time operator splitting and space adaptive multiresolution in the context of very localized and stiff reaction fronts. Based on recent theoretical studies of numerical analysis, such a strategy leads to a splitting time step which is not restricted neither by the fastest scales in the source term nor by restrictive diffusive step stability limits, but only by the physics of the phenomenon. We aim thus at solving accurately complete models including all time and space scales of the phenomenon, considering large simulation domains with conventional computing resources. The efficiency of the method is evaluated through 2D and 3D numerical simulations of a human ischemic stroke model, conducted on a simplified brain geometry, for which a simple parallelization strategy for shared memory architectures was implemented, in order to reduce computing costs related to "detailed chemistry" features of the model.

Keywords: Reaction-diffusion, operator splitting, adaptive multiresolution, ischemic stroke, parallel computing

* This research was supported by a fundamental project grant from ANR (French National Research Agency - ANR Blancs) *Séchelles* (project leader S. Descombes) and by a CNRS PEPS Maths-ST2I project *MIPAC* (project leader V. Louvet).
** Ph.D. grant from Mathematics (INSMI) and Engineering (INSIS) Institutes of CNRS and supported by INCA project (National Initiative for Advanced Combustion).

1 Introduction

Numerical simulations of multi-scale phenomena are commonly used for modeling purposes in many applications such as combustion, chemical vapor deposition, or air pollution modeling. In general, all these models raise several difficulties created by the large number of unknowns and the wide range of temporal scales due to large and detailed chemical kinetic mechanisms, as well as steep spatial gradients associated with very localized fronts of high chemical activity. Furthermore, a natural stumbling block to perform 3D simulations is the unreasonable memory requirements of standard numerical strategies for time dependent problems.

The most natural idea to overcome these difficulties is to use dedicated numerical methods and to solve the complete models where diffusion, reaction and eventually convection are coupled together. One aims at solving strongly coupled nonlinear systems with either a fully implicit method, or yet semi-implicit or linearized implicit methods instead (see [6] and references therein). However, the strong stability restrictions for the latter when dealing with very fast temporal scales, as well as the computing cost and the huge memory requirements of these methods, even if adaptive grids are used, make these strategies difficult to be handled.

An alternative numerical strategy is then to combine implicit and explicit schemes to discretize nonlinear evolution problems in time. Further studies settled the appropriate numerical background for these methods called IMEX, which in particular might be conceived to solve stiff nonlinear problems [19, 16]. These methods are usually very efficient. Nevertheless, on the one hand, the feasibility of utilizing dedicated implicit solvers over a discretized domain becomes soon critical when treating large computational domains. And on the other hand, the time steps globally imposed over partial regions or the entire domain are strongly limited by either the stability restrictions of the explicit solver or by the fastest scales treated by the implicit scheme.

However, in many multi-scale problems, the fastest time scales do not play a leading role in the global physical phenomenon and thus, we might consider the possibility of using reduced models where these chemical scales have been previously relaxed. These simplified models provide reasonable predictions and the associated computing costs are significantly reduced in comparison with comprehensive chemical models. Nevertheless, these reduced models provide only approximate solutions and are usually accessible when the system is well-partitioned and the fastest scales can be identified or isolated, a process that in realistic configurations, relies on sensitivity analysis which is most of the time difficult to conduct and justify.

It is then natural to envision a compromise, since the resolution of the fully coupled problem is most of the time out of reach and the appropriate definition of reduced models is normally difficult to establish. In this context, time operator splitting methods have been used for a long time and there exists a large literature showing the efficiency of such methods for evolution problems. In practice, it is firstly necessary to decouple numerically the reaction part from

the rest of the physical phenomena like convection, diffusion or both, for which there also exist dedicated numerical methods. Hence, these techniques allow a completely independent optimization of the resolution of each subsystem which usually yields lower requirements of computing resources.

In the context of multi-scale waves, the dedicated methods chosen for each subsystem are then responsible for dealing with the fast scales associated with each one of them, in a separate manner; then, the composition of the global solution based on the splitting scheme should guarantee an accurate description of the global physical coupling, without being related to the stability constraints of the numerical resolution of each subsystem. A rigorous numerical analysis is therefore required to better establish the conditions for which the latter fundamental constraint is verified. As a matter of fact, several works [20, 17, 6] proved that the standard numerical analysis of splitting schemes fails in presence of scales much faster than the splitting time step and motivated more rigorous studies for these stiff configurations [10, 9] and in the case where spatial multi-scale phenomena arise as a consequence of steep spatial gradients [8].

We therefore introduce a new operator splitting strategy, based on these theoretical results, that considers on the one hand, a high order method like Radau5 [13], based on implicit Runge-Kutta schemes for stiff ODEs, to solve the reaction term; and on the other hand, another high order method like ROCK4 [1], based on explicit stabilized Runge-Kutta schemes, to solve the diffusion problem. Exploiting the splitting configuration, a parallel computing technique is then implemented for the time integration stage, in the framework of shared memory computing architectures. Finally, the proposed numerical strategy is complemented by a mesh refinement technique based on Harten's pioneering work on adaptive multiresolution methods [14], being aware of the interest of adaptive mesh techniques for propagating waves exhibiting spatial multi-scale phenomena with steep gradients. The main goal is then to perform feasible and accurate in time and space simulations of the complete dynamics of multi-scale phenomena under study, with accuracy control of the solution and splitting time steps purely dictated by the physics of the phenomenon and not by any stability constraints associated with mesh size or source time scales.

The paper is organized as follows: In Section 2, we first recall the standard time operator splitting schemes to then describe the construction of an optimal operator splitting scheme for multi-scale problems, and its coupling with a suitable grid adaptation strategy, the space adaptive multiresolution technique [4, 15]. 2D and 3D simulations of a reaction-diffusion system modeling human ischemic strokes with a 19-species detailed chemistry [11], are presented in Section 3 to illustrate the potential and performance of the method. We end in section 4 with some concluding remarks and prospects.

2 Construction of the Numerical Strategy

In this section, we introduce a new splitting strategy for multi-scale waves modeled by stiff reaction-diffusion systems. Once established the time integration

strategy, we detail briefly the adaptive multiresolution method that we have implemented as mesh refinement technique for this new resolution technique.

2.1 Time Operator Splitting

Let us first set the general mathematical framework in this work. A class of multi-scale phenomena are modeled by general reaction-diffusion systems like:

$$\left.\begin{array}{ll} \partial_t \mathbf{u} - \partial_{\mathbf{x}} \left(\mathbf{D}(\mathbf{u}) \partial_{\mathbf{x}} \mathbf{u} \right) = \mathbf{f}\left(\mathbf{u}\right), \mathbf{x} \in \mathbb{R}^d, \ t > 0, \\ \mathbf{u}(0, \mathbf{x}) = \mathbf{u}_0(\mathbf{x}), \qquad\qquad\qquad \mathbf{x} \in \mathbb{R}^d, \end{array}\right\} \tag{1}$$

where $\mathbf{f} \ : \ \mathbb{R}^m \to \mathbb{R}^m$ and $\mathbf{u} \ : \ \mathbb{R} \times \mathbb{R}^d \to \mathbb{R}^m$, with the diffusion matrix $\mathbf{D}(\mathbf{u})$, which is a tensor of order $d \times d \times m$.

In order to simplify the presentation, we consider problem (1) with linear diagonal diffusion, in which case the elements of the diffusion matrix are written as $D_{ijk}(\mathbf{u}) = D_k \delta_{ij}$, so that the diffusion operator reduces to the heat operator with scalar diffusion coefficient D_k for component u_k of $\mathbf{u}$, $k = 1, \ldots, m$. In any case, the proposed numerical strategy normally deals with general problem (1). Performing a fine spatial discretization, we obtain the semi-discretized initial value problem:

$$\left.\begin{array}{l} \dfrac{d\mathbf{U}}{dt} - \mathbf{B}\,\mathbf{U} = \mathbf{F}\left(\mathbf{U}\right), t > 0, \\ \mathbf{U}(0) = \mathbf{U}^0, \end{array}\right\} \tag{2}$$

where $\mathbf{B}$ corresponds to the discretization of the Laplacian operator with the coefficients D_k within; $\mathbf{U}$ and $\mathbf{F}\left(\mathbf{U}\right)$ are arranged component-wise all over the discretized spatial domain. Considering a standard decoupling of the diffusion and reaction parts of (2), we denote $\mathcal{X}^{\Delta t}(\mathbf{U}^0)$ as the numerical solution of the discretized diffusion equation:

$$\frac{d\mathbf{U}_D}{dt} - \mathbf{B}\,\mathbf{U}_D = 0, \quad t > 0, \tag{3}$$

with initial data $\mathbf{U}_D(0) = \mathbf{U}^0$ after an integration time step Δt. We also denote by $\mathcal{Y}^{\Delta t}(\mathbf{U}^0)$ the numerical solution of the reaction part:

$$\frac{d\mathbf{U}_R}{dt} = \mathbf{F}\left(\mathbf{U}_R\right), \quad t > 0, \tag{4}$$

with initial data $\mathbf{U}_R(0) = \mathbf{U}^0$.

The two Lie approximation formulae of the solution of system (2) are then defined by

$$\mathcal{L}_1^{\Delta t}(\mathbf{U}^0) = \mathcal{X}^{\Delta t}\mathcal{Y}^{\Delta t}(\mathbf{U}^0), \quad \mathcal{L}_2^{\Delta t}(\mathbf{U}^0) = \mathcal{Y}^{\Delta t}\mathcal{X}^{\Delta t}(\mathbf{U}^0), \tag{5}$$

whereas the two Strang approximation formulae [18] are given by

$$\mathcal{S}_1^{\Delta t}(\mathbf{U}^0) = \mathcal{X}^{\Delta t/2}\mathcal{Y}^{\Delta t}\mathcal{X}^{\Delta t/2}(\mathbf{U}^0), \quad \mathcal{S}_2^{\Delta t}(\mathbf{U}^0) = \mathcal{Y}^{\Delta t/2}\mathcal{X}^{\Delta t}\mathcal{Y}^{\Delta t/2}(\mathbf{U}^0), \tag{6}$$

where Δt is now the splitting time step. It is well known that Lie formulae (5) (resp. Strang formulae (6)) are approximations of order 1 (resp. 2) of the exact solution of (2) in the case where $\mathcal{X}^{\Delta t}$ and $\mathcal{Y}^{\Delta t}$ are the exact solutions $X^{\Delta t}$ and $Y^{\Delta t}$ of problems (3) and (4). Then, appropriate numerical approximations of $X^{\Delta t}$ and $Y^{\Delta t}$ are required in order to compute Lie and Strang formulae with the prescribed order.

Higher order splitting configurations are also possible. Nevertheless, the order conditions for such composition methods state that either negative time substeps or complex coefficients are necessary (see [13]). The formers imply normally important stability restrictions and more sophisticated numerical implementations. In the particular case of negative time steps, they are completely undesirable for PDEs that are ill-posed for negative time progression.

2.2 Time Integration Strategy

The standard orders achieved with a Lie or Strang scheme are no longer valid when we consider very stiff reactive or diffusive terms (see [10]). Furthermore, if the fastest time scales play a leading role in the global physics of the phenomenon, then the solution obtained by means of a splitting composition scheme will surely fail to capture the global dynamics of the phenomenon, unless we consider splitting time steps small enough to resolve such scales.

In the opposite case where these fast scales are not directly related to the physical evolution of the phenomenon, larger splitting time steps might be considered, but order reductions may then appear due to short-life transients associated to the fast variables. This is usually the case for propagating reaction waves where for instance, the speed of propagation is much slower than the chemical scales. In this context, it has been proved in [10] that better performances are expected while ending the splitting scheme by the time integration of the reaction part (4) or in a more general case, the part involving the fastest time scales of the phenomenon (see a numerical case in [9]). In particular, in the case of stiff reaction-diffusion systems with linear diagonal diffusion, no order loss is expected for the $\mathcal{L}_2^{\Delta t}$ and $\mathcal{S}_2^{\Delta t}$ schemes when faster scales are present in the reactive term. However, one must also take into account possible order reductions coming this time from space multi-scale phenomena due to steep spatial gradients whenever large splitting time steps are considered, as analyzed in [8].

All these theoretical considerations give us some insight into the numerical behavior of splitting techniques and thus, help us to select among the various splitting alternatives, depending on the nature of the problem. Nevertheless, the choice of suitable time integration methods for each subsystem is mandatory not only to guarantee such theoretical descriptions but also to take advantage of the particular features of each independent subproblem in order to solve them as accurate as possible with reasonable resources, as it is detailed in the following.

Time Integration of the Reaction: Radau5. Radau5 [13] is not only an A-stable method, but also L-stable, so that very stiff systems of ODEs might

be solved without any stability problem. It considers also an adapting time step strategy which guarantees a requested accuracy of the numerical integration and at the same time, allows to discriminate stiff zones from regular ones; hence, smaller time steps correspond to stiffer behaviors. It is a high order method (formally of order 5, which at worst might be reduced to 3) and thus, all error coming from the time integration will be bounded by the one due to the splitting procedure itself.

Nevertheless, this high order method is achieved thanks to an implicit Runge-Kutta scheme, this means that in a general case, nonlinear systems must be solved throughout the time integration process. Even if the systems resolution tools are highly optimized (which are based on modified Newton's methods), these procedures become very expensive for large systems and important memory requirements are needed in order to carry out these computations. As a consequence, the size of the system of equations to be solved is terribly limited by the computing resources. However, in a splitting scheme context, we easily overcome this difficulty because the reactive term of (2) is a system of ODEs without spatial coupling. Therefore, a local approach node by node is adopted where the memory requirements are only set by the number of local unknowns, which normally does not exceed conventional memory resources. In particular, in a shared memory computing environment, a straightforward parallelization is accomplished in which each core solves successively one single node and where neither synchronization stages nor data exchange are needed among nodes.

Finally, precious computing time is also saved because the time integration step is only adapted at nodes where the reaction phenomenon takes place. For multi-scale reaction waves, this happens in a very low percentage of the spatial domain, normally only in the neighborhood of the wavefront. Therefore, larger time steps are considered at nodes with a chemistry at (partial) equilibrium. This would not be possible if we integrated the entire reaction-diffusion system (2) at once.

Time Integration of the Diffusion: ROCK4. If we now consider ROCK4 [1], we recall that one of the most important advantages of such method is its explicit character, hence the simplicity of its implementation. In fact, no sophisticated Linear Algebra tools are needed (no resolution of linear systems required) and thus, the resolution is based on simple matrix-vector products. Nevertheless, the computation cost relies directly on the requested quantity of such products, that is the number of internal stages s needed over one time integration step Δt. The memory requirements are also reduced as a consequence of its explicit scheme; nevertheless we must keep in mind that these requirements increase proportionally with the number of nodes considered over the spatial domain.

ROCK4 is formally a *stabilized* explicit Runge-Kutta method and such methods feature extended stability domain along the negative real axis.Therefore, in order to guarantee stability for a fixed time step Δt, the number of stages s needed is directly related to the spectral radius $\rho(\partial \mathbf{g}/\partial \mathbf{v})$ (considering a general

problem such as $\mathbf{v}' = \mathbf{g}(\mathbf{v})$), since it should verify:

$$0.35 \cdot s^2 \geq \Delta t \, \rho \left(\frac{\partial \mathbf{g}}{\partial \mathbf{v}}(\mathbf{v}) \right).$$

The method is then very appropriate for diffusion problems because of the usual predominance of negative real eigenvalues for which the method is efficiently stable. A very suitable example is the linear diagonal diffusion problem (3) with only negative real eigenvalues and constant spectral radius $\rho(\mathbf{B})$. In our particular applications, the diffusive phenomenon has a leading role of propagator of perturbations over the (partial) equilibrium nodes that result on excitation of the reactive schemes and thus, the propagation of the reaction wave. The resulting self-similar character implies that the number of stages needed will remain practically constant throughout the evolution of the phenomenon. The spectral radius must be previously estimated (for example, using the Gershgoring theorem or even numerically, as proposed by the ROCK4 solver by means of a nonlinear power method).

Once again, the implementation of this diffusion solver over the entire reaction-diffusion system (2) will not be appropriate under neither theoretical nor practical considerations, and highlights the inherited advantages of operator splitting. In particular, the resolution of diffusion problem (3) is also parallelized, that is, each core solves successively one single diffusion problem for only one specie, which yields an important reduction in the number of variables and consequently, in computing time. Finally, ROCK4 is also a high order method (order 4); therefore, the theoretical operator splitting analysis rest valid and the overall time integration errors are mainly due to the splitting scheme, where all the inner reaction and diffusion time scales are properly solved by these high order dedicated solvers.

2.3 Mesh Refinement Technique

We are concerned with the propagation of reacting wavefronts, hence important reactive activity as well as steep spatial gradients are localized phenomena. This implies that if we consider the resolution of reactive problem (4), a considerable amount of computing time is spent on nodes that are practically at (partial) equilibrium (see for example a precise computing time evaluation in [12]). Moreover, there is no need to represent these quasi-stationary regions with the same spatial discretization needed to describe the reacting wavefront, so that the diffusion problem (3) might also be solved over a smaller number of nodes. An adapted mesh obtained by a multiresolution process [4, 15] which discriminates the various space scales of the phenomenon, turns out to be a very convenient solution to overcome these difficulties.

Therefore, let us consider a set of nested spatial grids j with $j = 0, 1, \cdots, \mathrm{J}$ from the coarsest to the finest one. A multiresolution transformation allows to represent a discretized function as values on a coarser grid plus a series of local estimates at different levels of such nested grids. These estimates correspond

to the wavelet coefficients of a wavelet decomposition obtained by inter-level transformations, and retain the information on local regularity when going from a coarse to a finer grid. Hence, the main idea is to use the decay of the wavelet coefficients to obtain information on local regularity of the solution: lower wavelet coefficients are associated to local regular spatial configurations and vice-versa.

This representation yields to a thresholding process that builds dynamically the corresponding adapted grid on which the solutions are represented; then the error committed by the multiresolution transformation is proportional to ε, where ε is a threshold parameter [14, 5]. Finally, numerical experiments, based on this error estimate and on the splitting ones, allow one to properly choose the various simulation parameters used to predict the expected level of accuracy of the simulation. As a consequence, a more precise control of error can be drawn out of this optimal combination of methods.

2.4 Choice of Splitting Time Step

The splitting time step is set by the desired level of accuracy in the resolution of the wave speed, the wave profile, both, or any other parameter, depending on the problem and considering that each subsystem if perfectly resolved. It is thus only depending on the phenomenon we want to describe and therefore, on the degree of decoupling we can achieve between the various subsystems within a prescribed error tolerance. For instance, in this particular application, we have chosen a splitting time step Δt that verifies:

$$E_v = \frac{|v - v_{split}|}{v} \leq \eta_v, \tag{7}$$

where η_v is an accuracy tolerance for the velocity error E_v, considering a reference wave solution $\mathbf{u}$ of problem (1) with corresponding wavefront speed v, and the approximated solution $\mathbf{u}_{split}$ of speed v_{split}, computed by the operator splitting technique. Notice that in order to remain coherent with the previous constraint and also to guarantee an accurate resolution of the reaction and diffusion problems, the corresponding accuracy tolerances η_{Radau5} and η_{ROCK4} of these solvers must verify:

$$\eta_{Radau5}, \eta_{ROCK4} < \eta_v. \tag{8}$$

Finally, taking into account that the time evolution is performed on an adapted grid, fixed during each time step, the resulting splitting time step should verify a CFL-like condition:

$$\Delta t \leq \frac{n \Delta x}{v_{split}}, \tag{9}$$

where Δx corresponds to the spatial discretization at the finest grid and $n \geq 2$ considers the standard refinement criterion that enlarges uniformly the refined region obtained by the multiresolution technique [14]. This CFL-like condition is used to verify that the locally refined spatial gradients remain into the finest regions during a time step evolution; this is required not because of stability

issues as for time integration of hyperbolic problems, but to guarantee the spatial accuracy of the approximation.

In the case of self-similar progression of wavefronts, the selection of the time step is simplified by the fact that usually it does not need to be computed more than once. Let us underline that the proposed procedure has been designed in such a way that, in case one is able to estimate such a splitting time step at any computed time based on error control at a given tolerance, then the numerical strategy can be used exactly as it is provided with a dynamical self-adapted splitting time step for more general unsteady solutions of reaction-diffusion and convection-reaction-diffusion systems of equation [7].

3 Numerical Simulations

In this last section, we present some numerical illustrations of the proposed strategy. The performance of the method is discussed in the context of 2D and 3D simulations of a human ischemic stroke model which is briefly presented in what follows.

3.1 Ischemic Stroke Model

The model is based on a reaction-diffusion system of type (2) and considers ionic movements, glutamate excitotoxicity, cytotoxic edema and spreading depressions [11]. It focuses on the first hour of a stroke, when the ionic exchanges are the main mechanisms leading to cell death. Brain tissue is composed of two cell types, namely neurons and glial cells, and of extracellular space. In general, two domains are considered: the white and the grey matter which differ in their glial cell composition (astrocytes in grey matter and oligodendrocytes in white matter), and in their neuronal area composition (neuronal somas in grey matter and neuronal axons in white matter); nevertheless, in these simulations only grey matter will be taken into account. The ionic species considered are K^+, Na^+, Cl^-, Ca^{2+} and the Glutamate (glu). They pass through neuronal and glial membranes via ionic channels (such as voltage-gated channels, receptor-channels, stretch-channels) and via ionic pumps and transporters (which are energy-dependent). Finally, the model considers the following variables, dependent from both coordinates and time:

1. Volume fractions f_n and f_a (by brain volume unit) of neurons and glial cells. Extracellular volume fraction is thus given by $1 - f_n - f_a$.
2. Membrane potentials V_n and V_a of neurons and glial cells.
3. Concentrations of K^+, Na^+, Cl^-, Ca^{2+} and glu for neurons, glial cells and extracellular space.

Consequently, one has to solve a reaction-diffusion system with $m = 19$ unknowns, noticing that there is no diffusion for 9 variables: f_n, f_a, V_n, V_a and ions in neurons. There are no fluxes of ions in and out of the brain and thus, the boundary conditions are of Neumann homogeneous type. A stable

equilibrium solution is taken as initial condition $\mathbf{U}(0)$. For the moment, only simplified geometries can be simulated (see [12] for simulations on realistic brain geometries).

Let us finally remark that the reaction term $\mathbf{F}(\mathbf{U})$ is extremely stiff. In fact, the numerical computation of the Jacobian matrix $\partial\mathbf{F}/\partial\mathbf{U}$ near a stable stationary value $\mathbf{F}(\mathbf{U}) = 0$, gives negative eigenvalues with negligible imaginary parts but with real parts going from -10^8 to about -1. Moreover, it is impossible to separate fast and slow variables and even if this was possible, the voltage dependent gates would make this separation very local in time and space. All of these complex and stiff mechanisms yield a "detailed chemistry" description of the phenomenon.

3.2 2D Configuration

We first consider a computational domain of $[0, 5] \times [0, 5]$ (cm) and simulate the phenomenon over one hour $t \in [0, 3600]$ seconds. In what follows, we will refer to three ways to solve (2): the *quasi-exact* resolution, which considers the coupled reaction-diffusion problem (2) on an uniform mesh, computed by Radau5 with very fine tolerances; the *splitting* resolution, which uses the RDR Strang $\mathcal{S}_2^{\Delta t}$ scheme with Radau5 for the time integration of the reaction term and ROCK4 for the diffusive part, also on an uniform grid; and the proposed *MR/splitting* strategy, with the same $\mathcal{S}_2^{\Delta t}$ time integration scheme on an adapted mesh. All the computations have been performed on a 8 core (2x4) 64 bits machine (AMD Shanghai processors) of 2.7 GHz with memory capacity of 32 Gb.

In the following examples, the splitting time step was set to 10 and the threshold parameter $\varepsilon = 10^{-2}$; on the one hand, this splitting time step gives reasonable accurate resolutions for a realistic brain geometry, compared to real magnetic resonance (MR) images [12]; and on the other hand, this threshold value yields a normalized L^2-error $\lessapprox 10^{-2}$ between *splitting* and *MR/splitting* resolutions for all 19 variables.

Considering several values of J, the number of nested dyadic grids, figure 1 shows some *MR/splitting* results for the concentration of K^+ in the neurons at final time $t = 3600s$, for a spatial resolution equivalent to 256^2 (J = 8), 512^2 (J = 9), and 1024^2 (J = 10) grid points. One can clearly see that higher spatial discretizations yield better resolution of both the wave velocity and the dynamics of the wavefront; in particular, at least 512^2 points are needed in order to get a reasonably fine description of the phenomenon. A *quasi-exact* resolution with this level of discretization is already very expensive. Figure 2 shows the corresponding adapted grids for 256^2 and 1024^2: the refinement takes place only where it is required.

A preliminary study allows to choose the appropriate splitting time step according to §2.4. Figure 3 shows the propagation of the wavefront along x-axis across the core of the initial perturbation (see Figure 1), and the corresponding wave speed computed by the *splitting* strategy with splitting time steps going from 1 to 100 on an uniform grid of 1024^2. Smaller time steps imply naturally a more accurate description of the global phenomenon, measured in this case

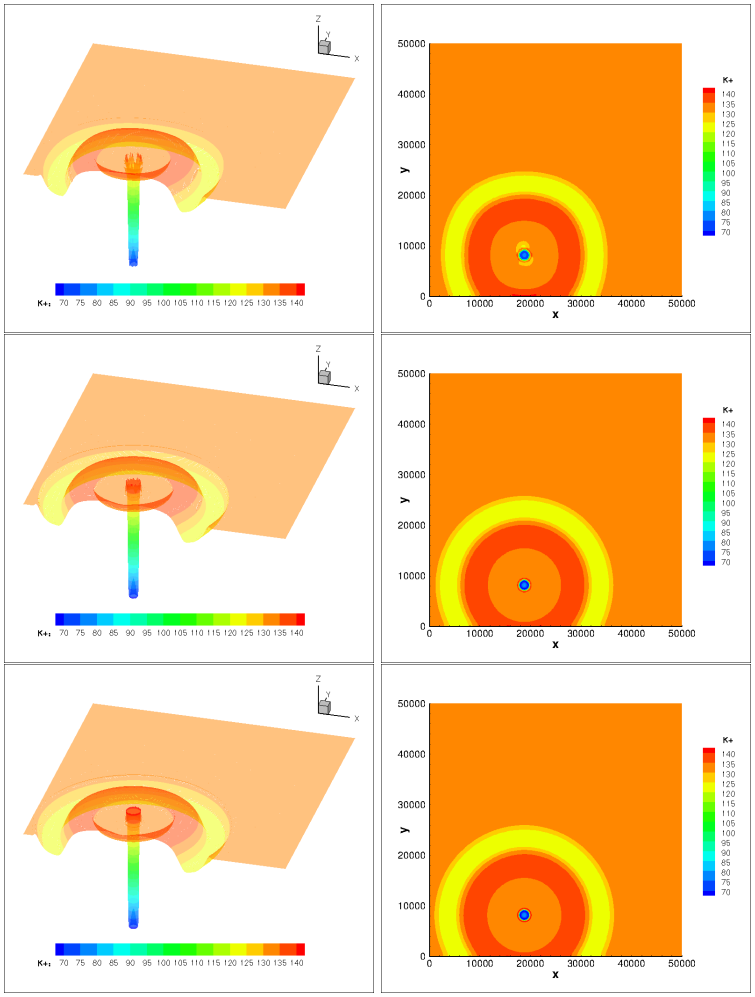

Fig. 1. K^+ in the neurons at 3600s for a 2D mesh of 256^2 (top), 512^2 (center) and 1024^2 (bottom) with $\varepsilon = 10^{-2}$.

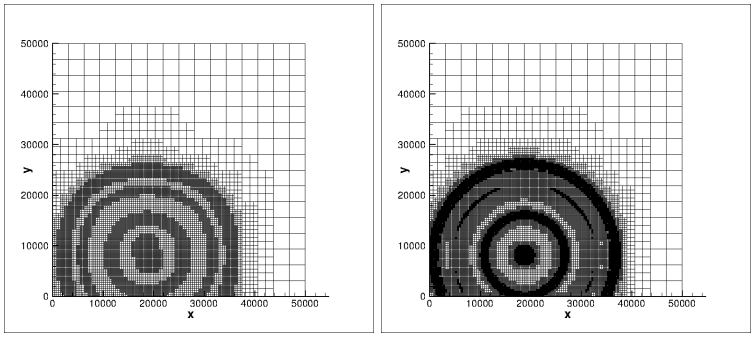

Fig. 2. 2D adapted meshes corresponding to 256^2 (left) and 1024^2 (right) spatial discretizations at the finest grid at 3600s.

by means of the wavefront speed, and show convergence towards the exact wave velocity v associated with problem (1). The chosen $\Delta t = 10$ implies a relative error of $\approx 3.8\%$ with $\eta_v = 5.10^{-2}$ into (7), with reference velocity of $v \approx 5.07$ once the propagating front is fully developed ($t \gtrsim 700s$). Similar results were obtained while considering propagation along y-axis. Tolerances of the solvers were set to $\eta_{Radau5} = 10^{-5}$ and $\eta_{ROCK4} = 10^{-7}$, after numerical experiments.

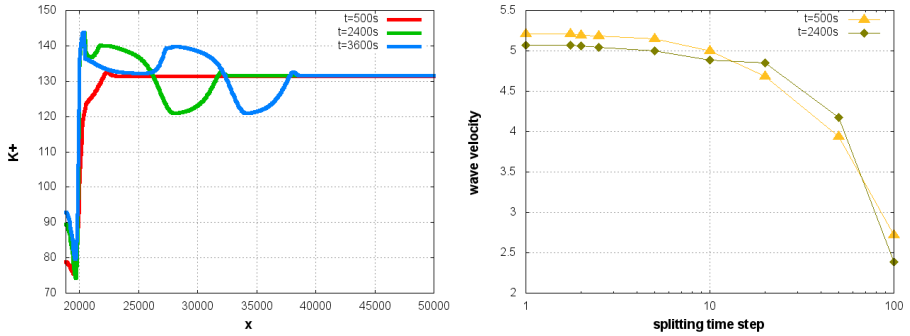

Fig. 3. Time evolution of K^+ in the neurons along x-axis (left) and corresponding wave velocities (right), obtained by *splitting* resolution on an uniform grid of 1024^2.

For this particular problem and with the selected Δt, the CFL-like condition (9) is verified for all $\Delta x \geq (10 \times 4.88)/2 = 24.4$, that is up to ~ 2049 points in each dimension, considering $v_{split} \approx 4.88$ and $n = 2$; therefore, this choice of the splitting time step is really consistent and avoids any kind of refinement problem for a wide range of spatial discretizations. Anyway, this is a rather conservative estimate because the numerical tests show that the refined zones during a time

step imply normally more than 2 cells, mainly due to the extended stencils obtained by graduation of the tree structure in multidimensional configurations.

Table 1 summarizes the computing times (CT) of the simulations, performed with 8 cores in parallel, and the gain of parallelization (GP) which is defined as the ratio between the computing time given by one single processor and the 8 cores in parallel. We see a rather high GP ($\max \mathrm{GP} = 8$) even though only the time integration procedure is parallelized: in fact, for this kind of stiff problems, the multiresolution operations take normally less than 5% of the total time consumption. Let us also remark that the parallelization of the reaction is practically optimal in the context of shared memory architectures because each core takes a new node immediately after finishing the previous one, without any need of synchronizing or exchanging data with the other cores. On the other hand, even though the parallelization of the diffusion is still very basic and not very efficient, it has a really low impact on the global performance of the method, considering that one reaction step takes ~ 10 times a diffusion one.

Table 1 includes also the achieved data compressions (DC), which is defined as one minus the ratio between the number of cells on the adapted grid (AG) and those on the finest uniform grid (FG), expressing the whole as a percentage:

$$\mathrm{DC} = \left(1 - \frac{\mathrm{AG}}{\mathrm{FG}}\right) \times 100. \tag{10}$$

Data compression increases with the number of levels as the space scales present in the problem are better discriminated by finer spatial resolutions.

Table 1. 2D case. Computing time (CT), gain of parallelization (GP), data compression (DC) and number of cells on the adapted grid (AG) for $\varepsilon = 10^{-2}$, various finest grids (FG) and levels of refinement (J).

FG	J	CT (min)	GP	AG (1000s)	DC (1000s)	AG (3600s)	DC (3600s)
256^2	8	12.60	7.32	4087	93.77	16312	75.11
512^2	9	42.96	7.20	9388	96.42	34315	86.91
1024^2	10	127.91	7.25	20527	98.04	72922	93.05

If we consider a *splitting* resolution on an uniform grid of 1024^2 and the corresponding *MR/splitting* strategy with $\varepsilon = 10^{-2}$, a reaction time integration step for the latter involves from 3% ($t = 100s$) to 27% ($t = 3600s$) of the computing time used in the first approach. This shows clearly the important amount of integration time wasted at (partial) equilibrium nodes for a standard non adapted grid strategy.

In order to take into account the memory requirements of each resolution strategy for a fine spatial resolution of 1024^2, we estimate the array size of the working space needed by Radau5 and ROCK4:

1. Radau5: $L_1 = 4 \times W_1 \times W_1 + 12 \times W_1 + 20$ (from [13]);

2. ROCK4: $L_2 = 8 \times W_2$ (from [1]);

where W_1 and W_2 are the number of unknowns solved by Radau5 and ROCK4. In the case of an uniform mesh, the total number of unknowns is $W = 19 \times 1024^2 \approx 1.99 \times 10^7$ and thus, the global size L required for each solver is:

1. *Quasi-exact*: $W_1 = W \approx 1.99 \times 10^7$ and $L = L_1 \approx 1.6 \times 10^{15}$.
2. *Splitting*: $W_1 = 19, W_2 = 10 \times W/19 \approx 1.05 \times 10^7$ and $L = L_1 + L_2 \approx 8.4 \times 10^7$.
3. *MR/Splitting* with $\varepsilon = 10^{-2}$: $W_1 = 19$, $W_2 = 0.07 \times 10 \times W/19 \approx 7.34 \times 10^5$ and $L = L_1 + L_2 \approx 5.9 \times 10^6$; with minimum data compression of 93%.

Considering a standard platform on which each double precision value is represented by 64 bits, each solver shall require 90.9 Pb, 5.0 Gb and 360.1 Mb.

3.3 3D Configuration

Let us consider now a 3D configuration with the same parameters as in the previous 2D case, in a space region of $[0,5] \times [0,5] \times [0,5]$ (cm). In order to explore the feasibility and potential advantages of the method, let us consider two cases with 8 and 9 nested dyadic grids, corresponding to 256^3 and 512^3 cells on the finest grid J. For the first case of 256^3, the achieved data compression DC goes from 99.00%, 95.93% and 87.23% at times 1000s, 2000s and 3600s, respectively; the computing time CT was of about 21.83 hours with a gain of parallelization GP of 6.99.

Figure 4 shows the concentration of K^+ in the neurons and the corresponding adapted grids at 1000s (DC = 99.26%) and 2000s (DC = 96.73%) for the 512^3 case; CT $\approx$ 37.41 hours for $t \in [0, 2000]$ (s) and GP = 7.05. Longer simulations times yield larger simulation domains which are not longer feasible with the considered computing resource at least in a shared memory environment, and the current state of development of the code.

Performing the same comparison concerning memory requirements, the total number of unknowns for the second case is $W = 19 \times 512^3 \approx 2.55 \times 10^9$ and the global size of L required by each solver is:

1. *Quasi-exact*: $W_1 = W \approx 2.55 \times 10^9$ and $L = L_1 \approx 2.6 \times 10^{19}$.
2. *Splitting*: $W_1 = 19$, $W_2 = 10 \times W/19 \approx 1.34 \times 10^9$ and $L = L_1 + L_2 \approx 1.1 \times 10^{10}$.
3. *MR/Splitting* with $\varepsilon = 10^{-2}$: $W_1 = 19$, $W_2 = 0.04 \times 10 \times W/19 \approx 5.37 \times 10^7$ and $L = L_1 + L_2 \approx 4.3 \times 10^8$; with minimum data compression of 96%.

Therefore, each solver shall require at least 1.4 Zb, 655.7 Gb and 25.6 Gb of memory capacity.

4 Conclusions

The present work proposes a new numerical approach which is shown to be computationally efficient. It couples adaptive multiresolution techniques with a

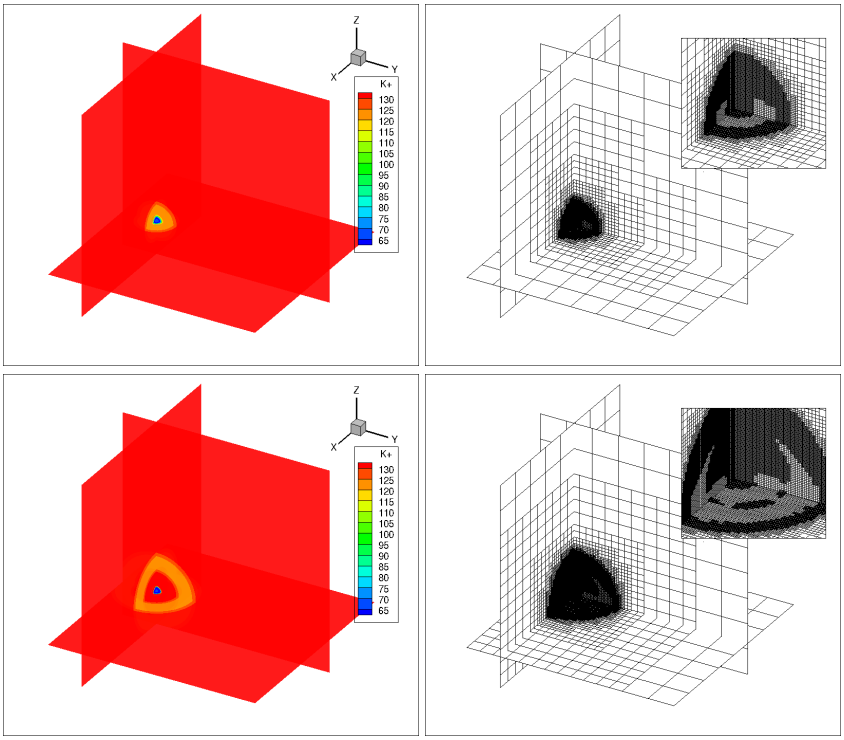

Fig. 4. 3D case. K^+ in the neurons (left) and corresponding adapted grids (right) at $1000s$ (top) and $2000s$ (bottom) with $\varepsilon = 10^{-2}$. Finest grid: 512^2.

new operator splitting strategy for multi-scale reactions waves modeled by stiff reaction-diffusion systems. The splitting time step is chosen on the sole basis of the structure of the continuous system and its decoupling capabilities, but not related to any stability requirement of the numerical methods involved in order to integrate each subsystem, even if strong stiffness is present. The technique considers on the one hand, dedicated high order time integration methods to properly solve the entire spectrum of temporal scales of both the reaction and the diffusion part; and on the other hand, an adaptive multiresolution technique to represent and treat more accurately local spatial gradients associated with the wave front. A straightforward parallelization technique was presented that shows also to be very efficient in the context of shared memory machines. The resulting highly compressed data representations as well as the accurate and feasible resolution of these stiff phenomena prove that large computational domains previously out of reach can be successfully simulated with conventional computing resources, in this case a single and standard workstation.

We have focused our attention on reaction-diffusion systems in order to settle the foundations for simulation of more complex phenomena with fully convection-reaction-diffusion systems or even more detailed models such as com-

bustion with complex chemistry. In particular, a major contribution of this work is related to the fact that we provide an error control in both space and time of the solution, once the splitting time step for the continuous system of PDEs is defined in order to respect a given tolerance compared to the coupled solution. So far, since we have investigated reaction waves, this time step is evaluated once for all and does not need to be re-evaluated dynamically during the simulation, even though an extended self-adapting time step procedure have been recently developed by the authors for more general unsteady problems [7].

However, an important amount of work is still in progress concerning on the one hand, programming features such as data structures, optimized routines and parallelization strategies. For instance, some interesting investigations have recently addressed these issues very nicely [2, 3]. And on the other hand, numerical analysis of theoretical aspects, which may surely lead to better error estimates to extend and further improve the proposed numerical strategy. These are particular topics of our current research.

References

1. Abdulle, A.: Fourth order Chebyshev methods with recurrence relation. Society for Industrial and Applied Mathematics J. Sci. Comput. 23, 2041–2054 (2002)
2. Brix, K., Massjung, R., Voss, A.: A hash data structure for adaptive PDE-solvers based on discontinuous Galerkin discretizations. IGPM-Rep. 302, RWTH Aachen (2009)
3. Brix, K., Melian, S., Müller, S., Schieffer, G.: Parallelisation of multiscale-based grid adaptation using space-filling curves. ESAIM: Proc. 29, 108–129 (2009)
4. Cohen, A.: Wavelet methods in numerical analysis, vol. 7. Elsevier, Amsterdam (2000)
5. Cohen, A., Kaber, S., Müller, S., Postel, M.: Fully adaptive multiresolution finite volume schemes for conservation laws. Math. of Comp. 72, 183–225 (2003)
6. D'Angelo, Y.: Analyse et Simulation Numérique de Phénomènes liés à la Combustion Supersonique. Ph.D. thesis, Ecole Nationale des Ponts et Chaussées (1994)
7. Descombes, S., Duarte, M., Dumont, T., Louvet, V., Massot, M.: Adaptive time splitting method for multi-scale evolutionary PDEs. Accepted for Confluentes Mathematici (2011)
8. Descombes, S., Dumont, T., Louvet, V., Massot, M.: On the local and global errors of splitting approximations of reaction-diffusion equations with high spatial gradients. Int. J. of Computer Mathematics 84(6), 749–765 (2007)
9. Descombes, S., Dumont, T., Louvet, V., Massot, M., Laurent, F., Beaulaurier, J.: Operator splitting techniques for multi-scale reacting waves and application to Low Mach number flames with complex chemistry: Theoretical and numerical aspects. In preparation (2011)
10. Descombes, S., Massot, M.: Operator splitting for nonlinear reaction-diffusion systems with an entropic structure: Singular perturbation and order reduction. Numer. Math. 97(4), 667–698 (2004)
11. Dronne, M.A., Boissel, J.P., Grenier, E.: A mathematical model of ion movements in grey matter during a stroke. J. of Theoretical Biology 240(4), 599–615 (2006)

12. Dumont, T., Duarte, M., Descombes, S., Dronne, M.A., Massot, M., Louvet, V.: Simulation of human ischemic stroke in realistic 3D geometry: A numerical strategy. Submitted to Bulletin of Math. Biology, available on HAL (http://hal.archives-ouvertes.fr/hal-00546223) (2010)
13. Hairer, E., Wanner, G.: Solving ordinary differential equations II. Springer-Verlag, Berlin, second edn. (1996), Stiff and differential-algebraic problems
14. Harten, A.: Multiresolution algorithms for the numerical solution of hyperbolic conservation laws. Comm. Pure and Applied Math. 48, 1305–1342 (1995)
15. Müller, S.: Adaptive multiscale schemes for conservation laws, vol. 27. Springer-Verlag, Heidelberg (2003)
16. Shampine, L.F., Sommeijer, B.P., Verwer, J.G.: IRKC : An IMEX solver for stiff diffusion-reaction PDEs. J. Comput. Appl. Math. 196(2), 485–497 (2006)
17. Sportisse, B.: An analysis of operator splitting techniques in the stiff case. J. Comput. Phys. 161(1), 140–168 (2000)
18. Strang, G.: On the construction and comparison of difference schemes. SIAM J. Numer. Anal. 5, 506–517 (1968)
19. Verwer, J.G., Sommeijer, B.P., Hundsdorfer, W.: RKC time-stepping for advection-diffusion-reaction problems. J. Comput. Phys. 201(1), 61–79 (2004)
20. Verwer, J.G., Sportisse, B.: Note on operator splitting in a stiff linear case. Rep. MAS-R9830 (1998)